

Enhancement of Adhesion Between Copper Foil and Polyimide Film Containing Thermally Decomposable Polystyrene Particles

Mei-Hui Tsai,¹ Yi-Chia Huang,² I-Hsiang Tseng,¹ Hsin-Pei Yu,¹ Yin-Kai Lin²

¹Department of Chemical and Materials Engineering, National Chin-Yi University of Technology, Taichung 41101, Taiwan

²Department of Materials Science and Engineering, National Chiao Tung University, Hsinchu 30010, Taiwan

Received 5 October 2011; accepted 30 November 2011

DOI 10.1002/app.36615

Published online 25 April 2012 in Wiley Online Library (wileyonlinelibrary.com).

ABSTRACT: A facile method was developed to synthesize porous polyimide (PI) films with enhanced adhesion to Cu foil. Various amounts (0.1–4 wt %) of polystyrene (PS) spheres with the diameter of 250 nm were mixed with the PI precursor synthesized from pyromellitic dianhydride (PMDA) and 4,4'-oxydianiline in *N,N'*-dimethylacetamide. PS was decomposed during thermal imidization process to create the porous PI structure. The increase in surface area and surface roughness was observed from the obtained porous PI films and was a function of the PS content up to 4 wt

%. A significant improvement in the adhesion strength between porous PI film and Cu foil, which was determined by 90° peel test, was achieved. The adhesion strength of PI containing 4 wt % PS to Cu was 1.53 kgf/cm compared with pure PI of 1.08 kgf/cm. Meanwhile, the synthesized porous PI films exhibit sufficient mechanical strength and thermal stability for practical applications. © 2012 Wiley Periodicals, Inc. *J Appl Polym Sci* 126: E365–E370, 2012

Key words: porous polyimide; polystyrene; adhesion

INTRODUCTION

Printed circuit boards (PCBs) are micron-thin conducting circuits fabricated on dielectric boards for locating electronic devices. Compared with the traditional rigid ones, the advanced flexible PCBs (FPCBs) have many advantages in applications demanding more integrated electronic devices and roll-to-roll manufacture system. Polyimides (PIs) have good thermal stability, chemical resistibility, and excellent mechanical properties, such as low creep, low stress relaxation, high yield stress, and high tensile strength.^{1–7} For these reasons, metal-coated PI films are commonly used as FPCBs. To enhance the interfacial adhesion strength, an additional metal layer, chromium or nickel, is commonly deposited at the interface of Cu and PI films.^{8–10} Another approach to improve the interfacial adhesion strength is to produce the covalent bonding between metal layer and PI film by using coupling agents.³ The interfacial adhesion strength can also be enhanced by plasma treat-

ment.^{11,12} However, its long-term stability is not sufficient in practical applications.

In this study, a simple method was developed to synthesize porous PI films to increase the surface area and thus improve the adhesive strength between Cu foil and PI film. Commercially available monodispersed polystyrene (PS) spheres with the diameter of 250 nm were selected as porogen to create the porous structure and thus increase the surface area of PI. Various amounts (0.1–4 wt %) of PS spheres were mixed with the PI precursor poly(amic acid) (PAA), and PS will be decomposed during thermal imidization process in fabrication of PI structure. Notably, the porous PI films remain in favorable mechanical strength and thermal stability as the PI matrix was derived from practically used low-cost dianhydride and diamine monomers.

EXPERIMENTAL

Materials

The crosslinked PS spheres with an average diameter of 250 nm were acquired from Rohm and Haas (PA, USA). 4,4'-Oxydianiline (ODA) from Aldrich (MO, USA) was used without pretreatment. Pyromellitic dianhydride (PMDA) provided by Taimide Tech (Hsinchu, Taiwan). was recrystallized from acetic anhydride prior to use. *N,N'*-dimethylacetamide (DMAc) from Fluka (OH, USA) was dried overnight through molecular sieves.

Correspondence to: M.-H. Tsai (tsaimh@ncut.edu.tw).

Contract grant sponsors: Ministry of Economic Affairs, Taiwan, ROC (through the project on flexible polymeric materials for electronic application [99-EC-17-A-07-S1-120]) and National Science Council, Taiwan, ROC (through the project [99-2815-C-167-019-E]).

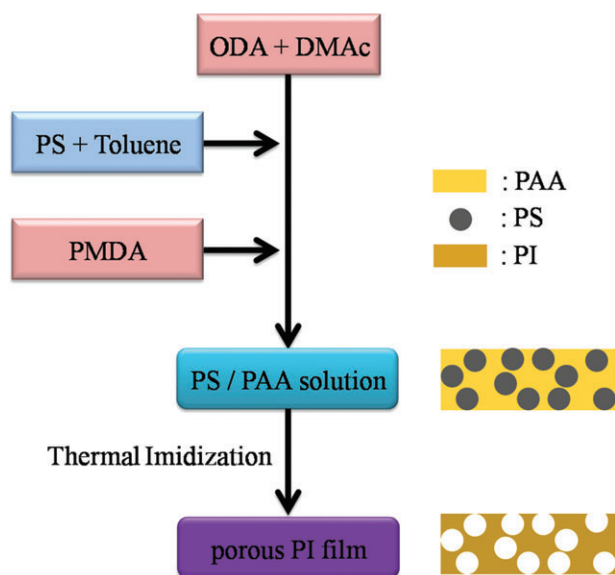


Figure 1 Reaction scheme for synthesizing porous PI films. [Color figure can be viewed in the online issue, which is available at wileyonlinelibrary.com.]

Preparation of PI films

To synthesize pure PI, 1.7231 g of ODA was first dissolved in 16.4 g of DMAc in a flask. Equimolar PMDA was then added to the above solution. The polymerization reaction was kept at room temperature for 2 h to produce a PAA solution. The resulting PAA solution was transformed into PI by thermal imidization at 350°C.

Preparation of porous PI films

The porous PI films were synthesized using ODA, PMDA, and PS spheres. The preparation procedure of porous PI films is shown in Figure 1. PS spheres were dispersed in 4.1 g of toluene and added into the ODA/DMAc solution in a flask. After the solution had been thoroughly stirred under N₂ atmosphere, 1.8769 g of PMDA was then mixed with the above solution. The obtained homogeneous PAA/PS solution was then coated on a glass substrate with a doctor blade and thermal imidized at 370°C for 2 h to produce porous PI films. The porous PI sample code was denoted PI-*x*, where *x* represents the wt % of added PS.

Measurements

Fourier transform infrared (FTIR) spectra of pure PI, PS, and porous PI films were obtained by using a FTIR spectrophotometer (Nicolet, Protégé-460). Field emission scanning electron microscopy (SEM, JEOL JSM-7401F) was acquired to observe the morphology of samples. Dynamic mechanical analysis (DMA) was conducted using a dynamic mechanical ana-

lyzer (TA Instruments, DMA 2980) to determine the storage modulus (E') and damping ($\tan \delta$) of samples. DMA experiments were performed in the tensile-film mode, at the frequency of 1 Hz and at the heating rate of 3°C/min from 60 to 300°C. The glass transition temperature (T_g) is defined as the maximum of $\tan \delta$ (E''/E'). The dimension stability of films was probed by a thermal mechanical analyzer (TMA, TA Instruments, Q400) at the heating rate of 10°C/min from 30 to 400°C. The coefficient of thermal expansion (CTE) of prepared films was characterized from TMA results of the dimension change over the temperature range of 100–200°C. To determine the thermal stability of films, thermal gravimetric analysis (TGA) was performed with a thermal gravimetric analyzer (TA Instruments, Q500) under N₂ or air using a heating rate of 20°C/min from 30 to 800°C for pure PI and porous PI. The TGA of PS was tested under air at the hearing rate of 20°C/min from 30 to 370°C and maintaining at 370°C for 2 h. The laminate of PI or porous PI film, adhesive, and Cu foil were fabricated under a pressure of 20 kg/cm² at 190°C for 5 min. The adhesion of the samples was examined by the 90° peel test method as shown in Figure 2, and the peel rate was 50.8 mm/min. The experimental values were the mean of at least 10 measurements. The morphology of laminates before and after peel test was investigated by an optical microscope (OM, Olympus, SZ-CTV) and an atomic force microscope (AFM, Veeco, D3100).

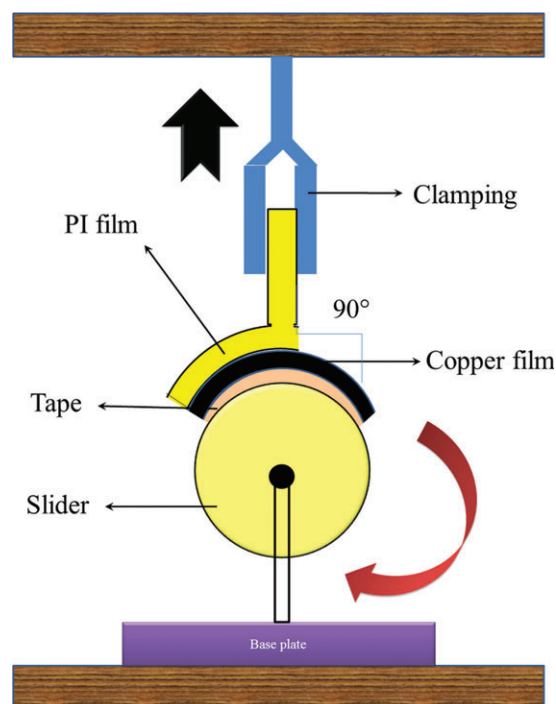


Figure 2 The diagram of peel test.³ [Color figure can be viewed in the online issue, which is available at wileyonlinelibrary.com.]

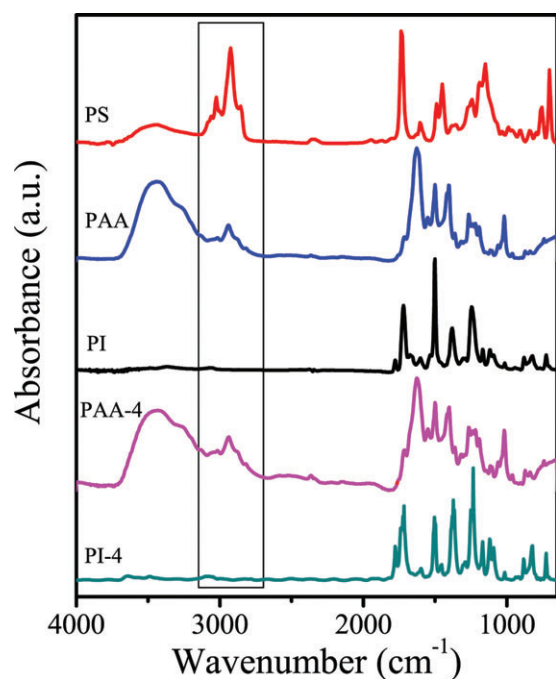


Figure 3 FTIR spectra of PS, PAA, pure PI, and porous PI films. PAA-4 is the precursor of PI-4. [Color figure can be viewed in the online issue, which is available at wileyonlinelibrary.com.]

RESULTS AND DISCUSSION

The FTIR spectra of PI and porous PI films are shown in Figure 3. The characteristic peaks of PI were observed at 1780 cm^{-1} (C=O asymmetric stretch), 1380 cm^{-1} (C–N stretch), 1720 cm^{-1} (C=O symmetric stretch), and 725 cm^{-1} (C=O bending),^{1–3,10} indicating the successful synthesis of PI structure. Figure 3 also shows the characteristic peaks of PS at 3010 cm^{-1} (C–H aromatic stretching vibration), 2921 cm^{-1} (C–H asymmetrical stretching vibration of CH_2), 2860 cm^{-1} (C–H asymmetrical stretching vibration of CH_2), and 755 cm^{-1} (C–H out-of-plane bending vibration of ring).¹³ The complete removal of PS during thermal imidization was confirmed by the FTIR results of PI-4 and PAA-4, where the characteristic peaks of PS disappeared after thermal imidization. Moreover, the TGA curve of PS under air was shown in Figure 4(a). The PS was apparently decomposed by increasing temperature to 370°C and completely decomposed with the following isothermal process at 370°C for 2 h. The TGA result indicates that the PS particles will be decomposed during the thermal imidization process.

SEM images of the surface of pure PI and porous PI-4 as well as the cross-section of PI-20 are shown in Figure 5(a–c). In this study, the difference in solubility parameters is only 0.1 indicating that PS can dissolve easily in toluene.^{14,15} However, the spherical PS particles are crosslinked such that PS chains remain in their spherical structure rather than disentangle and

freely stretch in toluene. The morphology confirms that the spherical pores on the surface or in the bulk of porous PI films have an average pore size of 250 nm. The presence of pores in PI films leads to a higher surface area of obtained films. Moreover, stronger adhesion strength between PI and copper will be achieved due to the anchor effect and fastener effect by mechanical interlocking theory.¹⁶ The image shown in Figure 5(d) is the surface of PI-4/Cu laminate after peel test. The residue of applied adhesive within pores of PI-4 indicates the improvement in the adhesive strength between porous PI and Cu. Figure 6 shows the AFM 3D image of the surfaces of PI and porous PI before and after peel test. A smooth surface was presented on pure PI as shown in Figure 6(a). In contrast, the pores are visible on Figure 6(c) for porous PI (PI-4). After peel test, the residue of adhesives presents on the surface of porous PI-4 as shown in Figure 6(d), which is consistent with the SEM images and the following OM images. Figure 7 shows OM images of the breaking side of PI or porous PI laminates after peel test. The residue of adhesive on the

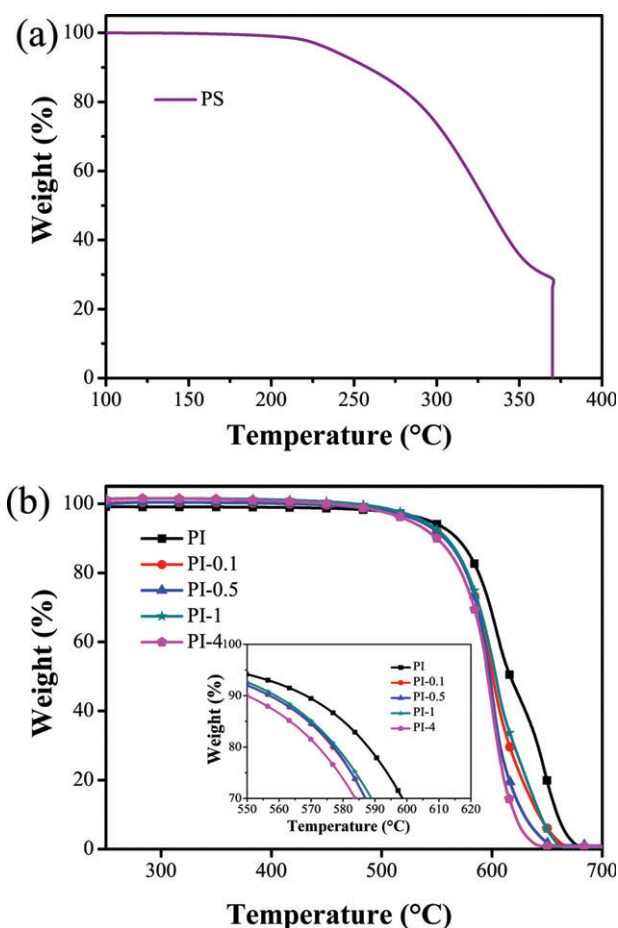


Figure 4 The thermogravimetric curves of (a) PS and (b) pure PI and porous PI films. [Color figure can be viewed in the online issue, which is available at wileyonlinelibrary.com.]

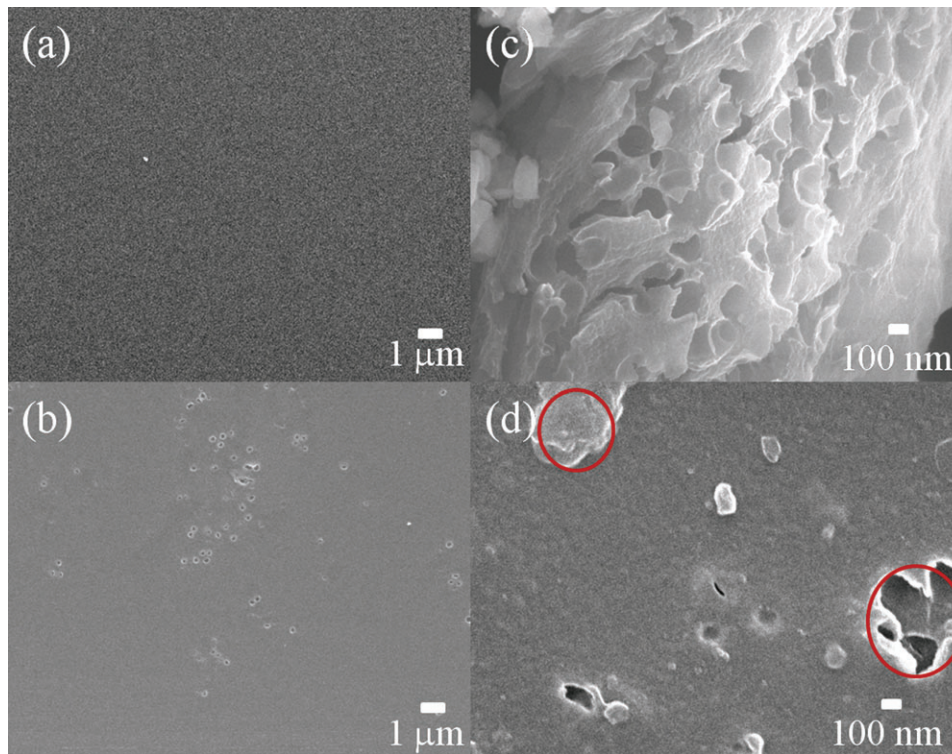


Figure 5 Morphology of (a) surface of PI, (b) surface of PI-4, (c) cross-section of PI-20, and (d) surface of PI-4 after peel test. The circles shown in (d) indicate the residue of adhesives within pores of PI after peel test. [Color figure can be viewed in the online issue, which is available at wileyonlinelibrary.com.]

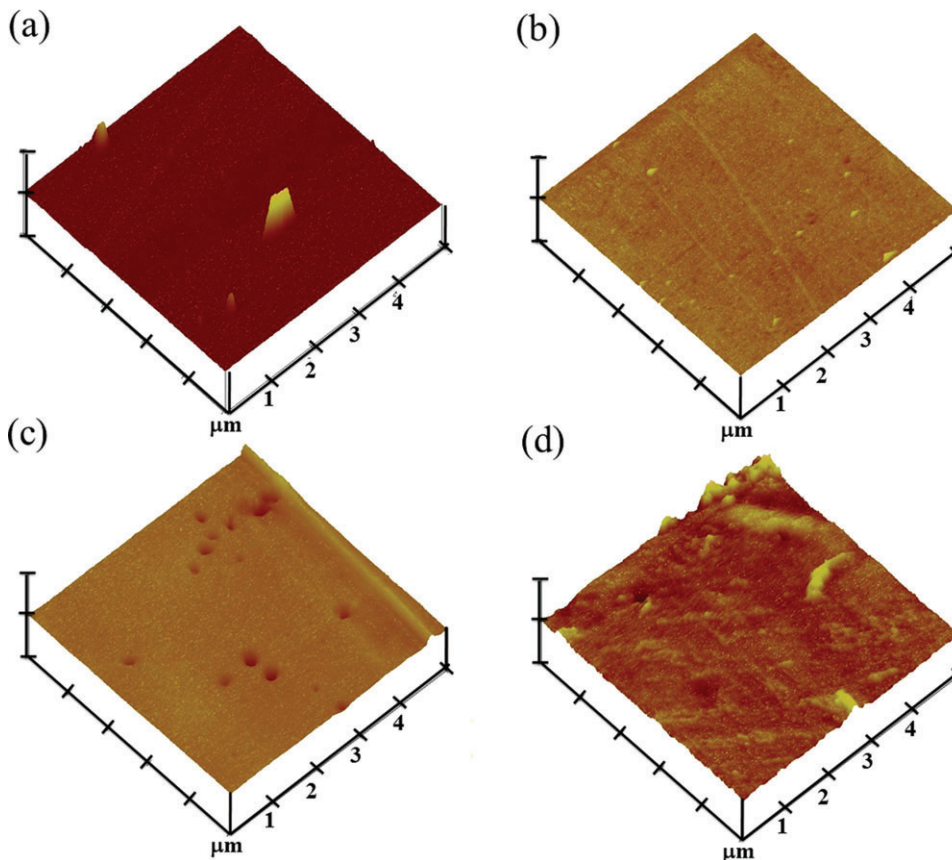


Figure 6 AFM 3D images of (a) pure PI, (b) pure PI after peel test, (c) porous PI-4, and (d) porous PI-4 after peel test. [Color figure can be viewed in the online issue, which is available at wileyonlinelibrary.com.]

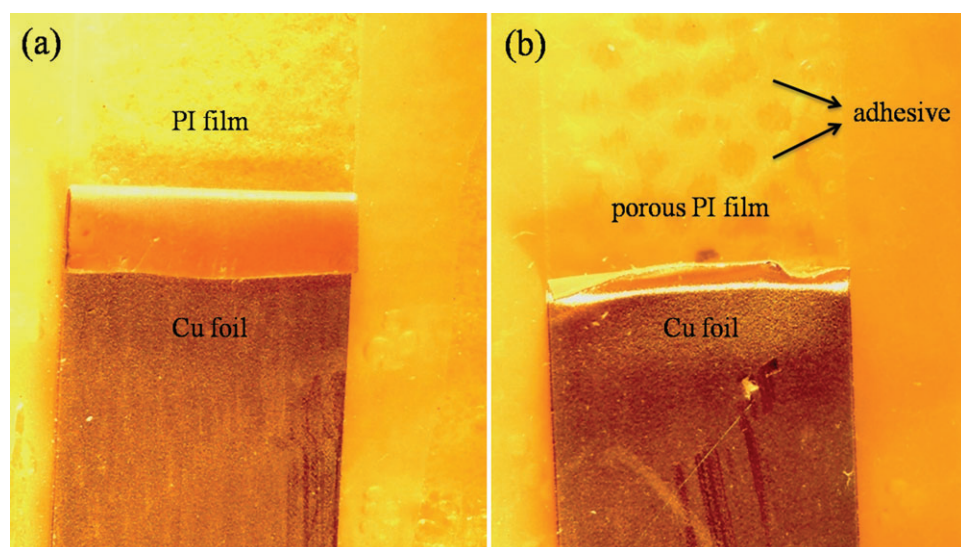


Figure 7 OM images of the breaking side of (a) PI film/adhesive/Cu foil laminate and (b) porous PI film/adhesive/Cu foil laminate. [Color figure can be viewed in the online issue, which is available at wileyonlinelibrary.com.]

breaking side of porous PI/Cu laminates is presented. The enhancement of adhesion is strongly associated with the presence of pores within PI matrix.

As shown in Table I, the adhesion strength between Cu and pure PI is 1.08 kgf/cm and increases significantly with the porosity of PI. The porous PI-4, which contains 4 wt % of PS, exhibits the adhesion strength of 1.53 kgf/cm. Based on those results, the peel strength of PI with Cu increases approximately 41.7% with every 1 wt % of PS addition in PI matrix. In previous study,³ the enhanced peel strength of relatively flexible PI matrix derived from 2,2'-bis[4-(4-aminophenoxy)phenyl]propane (BAPP) and 3,3',4,4'-benzophenonetetracarboxylic anhydride (BTDA) monomers was achieved by the addition of Al element. The highest peel strength was around 2 kgf/cm; however, the T_g of that PI system was relatively low (256°C). In this study, a more rigid PI matrix was formed from practically used monomers PMDA and ODA that the T_g value is much higher than previous one. As shown in Figure 8 and Table I, the T_g value of pure PI is

418°C and slightly decreases as the porosity in PI matrix increases. The T_g value of porous PI-4 is still as high as 400°C. Conversely, the damping ($\tan \delta$) intensity increases from 0.229 for pure PI to 0.257 for porous PI-4. The DMA results imply the slight increase in the flexibility of polymer chains in the porous films. The movement of PI chains in porous PI structure is easier than that in pure PI that a lower T_g value was observed from porous PI films. The higher damping in the $\tan \delta$ curve of porous PI suggests a closer packing of PI chains in porous PI matrix and thus a higher interaction force between molecular chains during chain movement.⁷

In addition, the CTEs of synthesized PI and porous PI films are determined from the dimension changes within the temperature range of 100–200°C. For porous PI, the CTE is in the range of 37–41 ppm/°C, which is slightly higher than that of pure PI, 32 ppm/°C. The TGA curves of PI and porous PI films are displayed in Figure 4(b) and the corresponding T_d values are designated at the temperature of 5% weight loss. The T_d values of porous PI

TABLE I
Mechanical, Thermal, and Adhesive Properties of Pure PI and Porous PI Films

Sample name	DMA		TMA	TGA	Peel strength (kgf/cm)
	T_g (°C) ^a	$\tan \delta$	CTE (ppm/°C) ^b	T_d (°C) ^c	
PI	418.2	0.229	32.4	543.9	1.08
PI-0.1	415.6	0.233	37.6	534.4	1.14
PI-0.5	411.9	0.238	40.0	534.5	1.24
PI-1	409.1	0.245	40.6	538.4	1.42
PI-4	397.4	0.257	41.2	525.7	1.53

^a The temperature at the peak of $\tan \delta$ curve is designated as T_g .

^b The thermal expansion coefficient (CTE) is determined over the temperature range of 100–200 °C.

^c The temperature at 5% weight loss is defined as the thermal decomposition temperature (T_d).

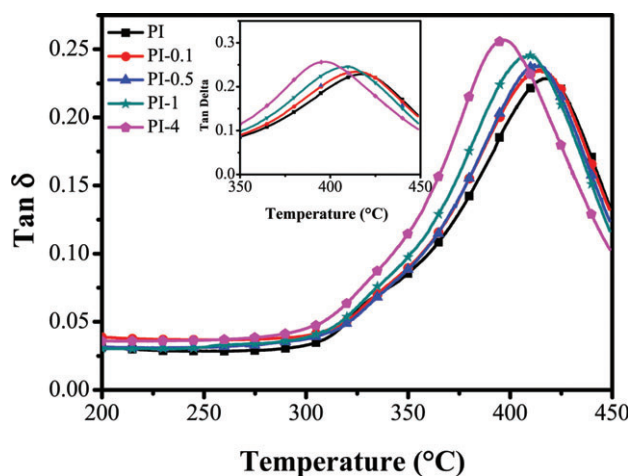


Figure 8 The $\tan \delta$ curves of pure PI and porous PI films. [Color figure can be viewed in the online issue, which is available at wileyonlinelibrary.com.]

films are all higher than 525°C, indicating the negligible effect of porosity on the thermal properties of resultant PI films.¹⁷

Compared with other literature, the improved adhesive strength in this study is relatively high and the method is relatively simple. For example, a complicated Xe or He plasma source ion implantation technique was applied to deposit Cu on PI films with improved adhesion of 0.35 or 0.25 kgf/cm, respectively.¹² The highest peel strength of Cu/Ni–Cu sputtered PI film, which was derived from the same monomers used in this study, was only 0.28 kgf/cm.⁸ The adhesion between fluorinated PI and silane/Cr-coated Cu foils was enhanced to 0.9 kgf/cm compared to 0.7 kgf/cm for PI/bare Cu foil.⁹ The peel strength of PI/Al nanocomposites element was significantly enhanced based on previous results; however, the thermal stability of PI was low.³ In contrast, the porous PI films fabricated by this facile method not only exhibit excellent adhesion to Cu foil but also present favorable mechanical strength and adequate thermal stability for FPCB applications.

CONCLUSIONS

The FTIR results confirm that the characteristic peaks of PS disappeared after thermal imidization,

indicating the complete removal of PS during thermal imidization. The porous structure of PI was proved from SEM and AFM images. The average pore size in porous PI is about 250 nm, which is consistent with the intrinsic particle size of added PS spheres. After peel test, the residue of adhesive presents on porous PI surface indicating an improved adhesive strength. The adhesive strength between PI and Cu foil significantly increases with the increasing amounts of PS in PI matrix. The adhesion strength between Cu foil and porous PI-4 is 1.53 kgf/cm compared to 1.08 kgf/cm for Cu/pure PI. The developed simple method successfully creates porous PI surface to dramatically enhance the adhesion strength to Cu foil.

References

1. Ghosh, M. K.; Mittal, K. L.; *Polyimides Fundamentals and Applications*; Marcel Dekker Press: New York, 1996.
2. Mittal, K. L. *Polyimides: Synthesis, Characterization and Applications*; Plenum Press: New York, 1991.
3. Tsai, M. H.; Lin, Y. K.; Chang, C. J.; Chiang, P. C.; Yeh, J. M.; Chiu, W. M.; Huang, S. L.; Ni, S. C. *Thin Solid Films* 2009, 517, 5333.
4. Wen, J.; Wilkes, G. L. *Chem Mater* 1996, 8, 1667.
5. Tsai, M. H.; Whang, W. T. *J Polym Res* 2001, 8, 77.
6. Delozier, D. M.; Orwoll, R. A.; Cahoon, J. F.; Johnston, N. J.; Smith, J. G.; Connell, J. W. *Polymer* 2002, 43, 813.
7. Tsai, M. H.; Whang, W. T. *J Appl Polym* 2001, 81, 2500.
8. Noh, B. I.; Yoon, J. W.; Lee, B. Y.; Jung, S. B. *J Mater Sci: Mater Electron* 2009, 20, 885.
9. Myung, B. Y.; Ahn, C. J.; Yoon, T. H. *J Appl Polym Sci* 2005, 96, 1801.
10. Hsiao, Y. S.; Whang, W. T.; Wu, S. C.; Chuang, K. R. *Thin Solid Films* 2008, 516, 4258.
11. Chin, J. W.; Wightman, J. P. *J Adhes* 1993, 41, 23.
12. Hong, J. H.; Lee, Y. H.; Han, S. H.; Kim, K. J. *Surf Coat Technol* 2006, 201, 197.
13. Bhutto, A. A.; Vesely, D.; Gabrys, B. J. *Polymer* 2003, 44, 6627.
14. Belmares, M.; Blanco, M.; Goddard, W. A.; Ross, R. B.; Caldwell, G.; Chou, S.-H.; Pham, J.; Olofson, P. M.; Thomas, C. J. *Comput Chem* 2004, 25, 1814.
15. Kiatkamjornwong, S.; Apiwattanong, S.; Rikukawa, M.; Ogata, N. *Colloids Surf A: Physicochem Eng Aspects* 1999, 153, 229.
16. McBain, J. W.; Hopkins, D. G. *J Phys Chem* 1925, 29, 188.
17. Fu, G. D.; Wang, W. C.; Li, S.; Kang, E. T.; Neoh, K. G.; Tseng, W. T.; Liaw, D. J. *J Mater Chem* 2003, 13, 2150.